Combust. Sci. Technol., 187: 1208–1228, 2015

ISSN: 0010-2202 print / 1563-521X online
DOI: 10.1080/00102202.2015.1027819

Taylor & Francis
Taylor & Francis Group

A ONE-DIMENSIONAL TRANSIENT SOLID FUEL CONVERSION MODEL FOR GRATE COMBUSTION OPTIMIZATION

Jorge Martinez-Garcia[1] and Thomas Nussbaumer[2]

[1]*Lucerne University of Applied Sciences and Arts, School of Engineering and Architecture, Horw, Switzerland*

[2]*Verenum Research, Zurich, Switzerland*

A one-dimensional transient model for simulating the conversion of solid biomass fuels in grate boilers is presented. The model considers drying; pyrolysis; and char oxidation; gas flow through the pore space of the bed; conductive, convective, and radiative heat transfer; and shrinkage of the fuel bed. It allows to study the influence of fuel properties and operating parameters on the solid fuel conversion, the resulting grate coverage, and the gas profiles. Experimental results from a 1.2 MW grate boiler at optimum conditions are used to adjust the moving bed velocity in the model. Calculations with increased fuel humidity then result in a prolonged drying time and unburned carbon in the ash. Adopted model runs further reveal that ideal conditions can be recovered either by increasing the excess air, by air pre-heating, or by reducing the boiler capacity. Hence, the model is useful to predict the influence of parameters on the fuel conversion, to evaluate measures for combustion optimization, and to develop control strategies.

Keywords: Combustion control; Combustion modeling; Fuel properties; Grate combustion; Grate coverage; Moving bed velocity; Part load operation

INTRODUCTION

To further increase the utilization of bioenergy, technologies enabling the use of solid biomass with high variability in moisture, ash, fuel size, and bulk density are of great interest. For such applications, grate boilers are suited and commonly applied. If the boiler operation is adjusted to the specific fuel, high burnout quality of the ash and the gases can be achieved. However, variations of the fuel characteristics remain a great challenge. In addition, pollutants from fuel constituents, such as nitric oxides from fuel nitrogen and particulate matter from ash constituents, need to be reduced by primary measures, which can be in target conflict to the burnout quality. Consequently, an in-depth understanding of the chemical and physical reactions of the solid fuel conversion on a grate and the subsequent gas phase reactions are needed. For this purpose, mathematical modeling and numerical simulations have been proved to be attractive approaches.

Received 29 October 2013; revised 6 March 2015; accepted 6 March 2015.

Address correspondence to Jorge Martinez-Garcia, Thermische Energiesysteme und Verfahrenstechnik, Technikumstrasse 21, Horw, Lucerne 6048, Switzerland. E-mail: jorgemartgarcia@gmail.com

Color versions of one or more of the figures in the article can be found online at www.tandfonline.com/gcst.

Relevant experience on modeling the solid fuel conversion process is available. Since the pioneering work of Essenhigh and Kuo (1970), models have become more sophisticated either in their description of the chemical and physical process or in the coupling between the bed and freeboard. A representative example is the two-dimensional (2D) transient model developed at the Sheffield University Waste Incinerator Center (SUWIC) (Yang et al., 2002, 2004), which later on lead to the development of the FLIC software. Perhaps the most sophisticated approach is the so-called discrete particle model (DPM) developed by Peters and coworkers (Peters, 2003) in which the thermal conversion process of a packed bed is accounted for by describing the process of each individual particle within the bed (Bruch et al., 2002; Peters, 2002; Peters and Bruch, 2003).

Fuel bed conversion is, in general, a transient 3D phenomena involving an assembly of solid particles embedded in a surrounding gas medium. However, for the situation on a moving grate with primary air fed through the grate and fuel transport along the grate, heat and mass transfer in the direction perpendicular to the grate, i.e., in the direction of the fuel bed height z, is dominant. Consequently, gradients of physical properties along the grate x and across the grate y are neglected; the solid conversion process in the bed can be modeled as a *transient* 1D phenomenon. This assumption is fairly fulfilled in typical moving grate boilers where the solid fuel exhibits far longer residence times than the gases, i.e., typically up to 1 h compared to seconds. Hence, this approach has been adopted by many authors in the literature.

Goh et al. (1998) developed a mathematical model for waste in a fixed bed, which predicts the evolution of the solid phase as well as both temperature and gas composition profiles (Goh et al., 2001). Shin and Choi (2000) presented a 1D transient model to better understand the combustion occurring inside a municipal solid waste (MSW) incinerator, which was validated in a column reactor at different air flow rates. Kær (2004b) proposed a 1D "walking column" approach to describe the fixed bed combustion of straw. The model predicts the existence of two distinct combustion modes observed at different air flow rate values and was used to generate the inlet conditions for CFD analysis of a 33-MW straw-fired grate boiler (Kær, 2004a). Di Blasi (2004) and Zhou et al. (2005) also simplified to one dimension a transient thermal conversion model in a fixed bed obtaining good agreement with experimental measurements. More recently 2D steady versions of a 1D transient model have been proposed to simulate the combustion of both MSW (Ashtana et al., 2010) and biomass (Troccia et al., 2012) on a traveling grate.

The described models enable one to calculate the solid fuel conversion and gas profiles under given conditions and present selected results for specific boundary conditions. However, information on the coverage of the grate with fuel, which has been experimentally identified as an important parameter for optimized operation of grate boilers with respect to ash slagging (Schroer et al., 2008) and pollutant emissions (Kiener and Nussbaumer, 2012) is scarce. Hence, detailed information applicable for grate design and control strategies for grate boilers for varying fuels and load situations is of interest for future developments.

In the present work a 1D transient model for the solid fuel conversion on a grate is presented that is suited for coupling with consecutive gas phase modeling and which enables the identification of the influence of the main design and operational parameters. Specific interest is given on air distribution and boiler capacity as well as on fuel parameters, such as moisture content and particle size. Special focus is given on the applicability of the model to optimize the design and the operation of grate boilers. For this purpose, the model is directly linked to input parameters resulting from the boiler design and operation, i.e., primary air ratio, primary air temperature, and boiler load. The applicability of the

model is illustrated by predicting fuel and operational parameter values at which optimum conditions for the fuel conversion on the grate are achieved. In addition, the effect of the moisture content on the gas profiles is illustrated.

THEORY

Modeling Approach

In the present model, the fuel bed is described as a continuous two-phase porous medium through which air from the bottom of the bed and gases from the fuel conversion flow. The solid phase consists of spherical fuel particles with specific properties, being initially homogeneous and of equal size. The particles are assumed to be thermally thin, i.e., with neglected internal temperature gradient. This assumption correctly represents the combustion behavior of a small single particle at high heating rate as found in pulverized coal combustion, while large particles of more than a few hundred microns react more slowly than predicted from isothermal models (Di Blasi, 1993; Lu et al., 2008). Consequently, effects from intraparticle gradients, such as the overlapping of moisture evaporation, devolatilization, and char burnout (Yang et al., 2005b) and widening of the reaction front (Johansson et al., 2007), are underestimated by the isothermal approximation. Nevertheless, in the case of solid fuel conversion under fixed bed conditions, the porous media model does not result in significant differences for particles smaller than 0.5 cm and enables reasonable approximations of the ignition rate and maximum temperatures with differences smaller than 15% for even bigger particles (Johansson et al., 2007). Hence, Yang et al. (2005) report on an example investigated with respect to controlling factors that particles smaller than 30 mm can be roughly regarded as thermally thin in the situation of packed bed combustion. Since the present work focuses on packed bed combustion with particles up to 20 mm, thermally thin particles are assumed. Therefore, continuous conservation equations can be applied in both phases in a more simple way using a 1D global coordinate system.

As the solid conversion proceeds, the solid phase loses mass by drying, pyrolysis, and char oxidation processes. This leads to a significant reduction of the bulk volume of the bed, which is here mathematically linked to the consumption of char by oxidation (Figure 1).

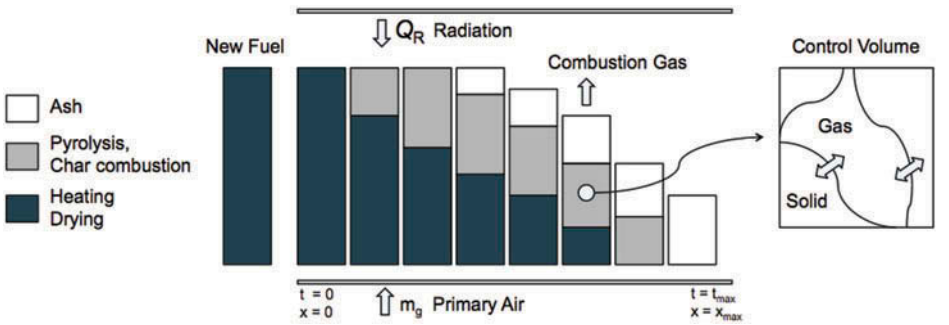

Figure 1 Schematic of the model. As a fuel column enters the grate, it receives radiation heat from the ceiling of the combustion chamber Q_R and primary air introduced from the bottom of the grate. As a consequence, the solid phase loses mass by drying, pyrolysis, and char oxidation processes leading to a reduction of the bed volume.

The evolution of the solid phase is here described by four scalar magnitudes, namely, density of moisture, density of dry wood, density of char, and solid temperature. The ash is assumed to remain as inner material in the bed. The gas phase, on the other hand, consists of oxygen, nitrogen, water vapor, carbon monoxide, carbon dioxide, gaseous volatiles, and tar (condensable organic compounds (COC)). This is described by scalar quantities accounting for the densities of the gas species and the gas temperature. All of these variables are considered simultaneously in the mass and energy balance partial differential equations system, which is solved to describe the local state of both phases.

Assumptions

To simplify the modeling, the calculations are performed based on the following assumptions:

- The pressure of the system is assumed to be constant at $p_0 = 1.013$ bar.
- Gases behave as ideal gases and are described by the ideal gas equation.
- Drying is assumed to occur at the evaporation temperature $T_{vp} = 373.15$ K.
- The fuel bed is described as a two-phase porous media and moves on the grate at constant velocity.
- The system is assumed to be one dimensional, hence gradients of physical properties along the grate are neglected.
- The solid phase loses mass via drying, pyrolysis, and heterogeneous char oxidation processes with a shrinking bed volume occurring during char oxidation only.
- The pyrolysis of dry wood is modeled by three parallel competing reactions for the transformation of wood into char, gas, and tar. Further, a secondary reaction for the formation of gas from tar is taken into account.
- For the conservation of solid components, transport mechanisms are neglected, so that their temporal variation is due to the source reaction term.
- Diffusion of gas species and momentum losses of gas by the fuel bed are neglected.

Governing Equations

For the solid phase, the governing equations are:
Continuity:

$$\frac{\partial(1-\epsilon_b)\rho_s}{\partial t} = R_{sg} \tag{1}$$

where ρ_s is the solid density, ϵ_b is the bed porosity, and R_{sg} is the net conversion rate from solid to gas due to drying, pyrolysis, and char combustion.

Solid components:

$$\frac{\partial(1-\epsilon_b)\rho_m}{\partial t} = R_m \tag{2}$$

$$\frac{\partial(1-\epsilon_b)\rho_w}{\partial t} = R_p \tag{3}$$

$$\frac{\partial(1-\epsilon_b)\rho_c}{\partial t} = R_{c^+} - R_{c^-} \tag{4}$$

Energy:

$$\frac{\partial(1-\epsilon_b)c_{ps}\rho_s T_s}{\partial t} = S_{cd} + S_{cv} + S_{rd} + \sum_i S_r k \tag{5}$$

For the gaseous phase, the governing equations are:

Continuity:

$$\frac{\partial \epsilon_b \rho_g}{\partial t} + \frac{\partial \epsilon_b v_g \rho_g}{\partial z} = -R_{sg} \tag{6}$$

Species transport:

$$\frac{\partial \epsilon_b \rho_i}{\partial t} + \frac{\partial \epsilon_b v_g \rho_i}{\partial z} = R_{g,i} \tag{7}$$

$$i = \mathrm{O_2},\ \mathrm{H_2O},\ \mathrm{CO},\ \mathrm{CO_2},\ \text{volatiles, tar}$$

Energy:

$$\frac{\partial\left(\epsilon_b c_{pg}\rho_g T_g\right)}{\partial t} + \frac{\partial\left(v_g \epsilon_b c_{pg}\rho_g T_g\right)}{\partial z} = S_{cd} - S_{cv} \tag{8}$$

State equation:

$$P = \frac{\rho_g \mathcal{R} T_g}{M_g} \tag{9}$$

where $\mathcal{R}$ is the universal gas constant and M_g is the mean molecular weight. The source terms R_i and S_i appearing in the above equations account, respectively, for the mass and energy loss/gain in both phases during the whole solid-gas conversion process. Expressions for such terms are listed in Table 1 and discussed in the following sections.

Main Reactions

Drying. Solid fuels, in particular biomass, contain a significant amount of moisture, which varies between 5% and 50% on dry basis (Yang et al., 2005a). Thus, drying may be of crucial importance to the solid conversion process in terms of both time and energy. In this work the drying process is modeled according to the constant evaporation approach (Collazo et al., 2012), where the rate of moisture release is given as expressed in Table 1, Eq. (20).

As can be seen, the rate of moisture evaporation R_m depends on the moisture evaporation enthalpy ΔH_m, the solid density ρ_s, and the solid specific heat c_{ps} at constant pressure. According to this approach, drying is assumed to occur at constant temperature ($T_{vp} =$ 373.15 K) and to be thermally controlled. Once a local region reaches the evaporation temperature T_{vp}, no variation of the temperature occurs and water vapor is emitted to the gas phase until the local moisture content is completely consumed.

Pyrolysis. Once the fuel is dried, the next reaction that occurs is pyrolysis. Several kinetic schemes for biomass pyrolysis, ranging from a simple one-step global model to

Table 1 Mass and energy source terms considered in the model

Mechanism	Volumetric rate	Equation
Drying: Wood → Stream / dry wood	$R_m = \begin{cases} -\frac{\rho_s c_{ps}}{\Delta H_m}\frac{\partial T_s}{\partial t}, & T_s \geq T_{vp} \\ 0 & T_s < T_{vp} \end{cases}$	(20)
Pyrolysis:	$R_p = -\Sigma_i R_i$	
Dry wood → Volatiles (v_1) / Tar (t) → Volatiles (v_2) / Char (c^+)	$R_i = A_i \exp[-E_i/\mathcal{R}T_s]$	(21)
	$i = (v_1,\ t,\ c^+)$	
Char Oxidation: $C + \frac{1}{\Theta}O_2 \rightarrow 2\left(1-\frac{1}{\Theta}\right)CO + \left(\frac{2}{\Theta}-1\right)CO_2$	$R_{c^-} = k_0\left(\frac{\rho o_2}{Mo_2}\right)\mathcal{R}T_g\rho_c$	(22)
Conduction	$S_{cd} = \frac{\partial}{\partial z}\left(\kappa_{eff}\frac{\partial T}{\partial z}\right)$	(23)
Convection	$S_{cv} = A_p h_t\left(T_s - T_g\right)$	(24)
Radiation	$S_{rd} = \xi\sigma A_p\left(T_{wall}^4 - T_s^4\right)$	(25)
Reaction	$S_{rk}^i = R_i \Delta H_i$	(26)

more complex approaches, have been proposed in the literature (Haseli et al., 2011). Pyrolysis is here considered through three parallel competitive reactions for the transformation of dry wood into gaseous volatiles, tar, and char, and a secondary reaction for the degradation of tar into volatiles, as sketched in Table. 1.

The total rate of decomposition of dry wood is given by Eq. (21), where ρ_w is the density of dry wood and the kinetic parameters $\{A_i,\ E_i\}$, $(i = v,\ t,\ c^+)$, for volatile (v), tar (t), and char production (c^+) are listed in Table 2. The kinetic data reported by Chan et al. (1985) is assumed for the three primary reactions, while for the secondary reaction the kinetic data reported by Liden et al. (1988) are used. The sign in Eqs. (20) and (21) expresses the fact that the mass is extracted from the solid phase.

Volatiles are considered to consist of CO, CO_2, H_2O, H_2, and CH_4, while tar and char are represented as benzene (C_6H_6) and pure carbon (C), respectively.

Char oxidation. The char produced from pyrolysis reacts with the oxygen provided by the primary air flow, yielding carbon monoxide (CO) and carbon dioxide (CO_2) in amounts that depend on the temperature. In this work the reaction scheme used by Zhou et al. (2005) and Van der Lans et al. (2000),

$$C + \frac{1}{\Theta}O_2 \rightarrow 2\left(1-\frac{1}{\Theta}\right)CO + \left(\frac{2}{\Theta}-1\right)CO_2$$

is considered. The stoichiometric factor $\Theta = (1 + 1/r_c)\,/\,(0.5 + 1/r_c)$ is expressed in terms of the ratio $r_c = CO/CO_2$, which is here estimated according to Yang et al. (2005a) as:

$$r_c = 2500\exp\left[-\frac{6420}{T_s}\right] \tag{10}$$

By considering the char oxidation to depend as a first-order reaction on the oxygen concentration, the overall char consumption rate can be written as Eq. (22) in Table 1,

where the overall coefficient k_0 depends on the competing between a chemical, $k_{ch} = A_c \exp(T_{ac}/T_s)$, and a diffusion, $k_d = (\mathrm{Sh}_B/d_p)\, D_{O_2-N_2}$, coefficient:

$$k_0 = \left(1/k_{ch} + \left(\mathcal{R}T_s\rho_c/\Phi M_c A_p\right)/k_d\right)^{-1} \tag{11}$$

In Eqs. (22) and (11), M_{O_2} and M_c are the molar mass of oxygen and carbon, respectively; $A_p = 6(1-\epsilon_b)/d_p$ is the specific particle's surface area; and d_p is the particle's diameter. The kinetic parameters A_c and T_{ac} are listed in Table 2, the diffusivity of oxygen in nitrogen, $D_{O_2-N_2}$, is given in Table 3, and the Sherwood number for the packed bed Sh_b is estimated using the analogy with convective heat transfer (Wakao and Funazkri, 1978) and the bed correction of Schlünder and Tsotsas (1988) as:

$$\mathrm{Sh}_b = [1 + 1.5\,(1-\epsilon_b)]\left[2 + 1.1\mathrm{Re}^{0.6}\mathrm{Sc}^{1/3}\right] \tag{12}$$

where $\mathrm{Sc} = \nu_g/(\rho_g d_p)$ and $\mathrm{Re} = (\rho_g \nu_g d_p)/\nu_g$ the are the Schmidt and the Reynolds numbers, respectively.

Table 2 Main properties of the fuel, thermal parameters, and kinetic data

Parameter	Value	Reference
Thermal conductivity [W/mK]		
Moisture: κ_m	0.58	(Portiero et al., 2007)
Dry wood: κ_w	0.20	(Portiero et al., 2007)
Char: κ_c	0.10	(Portiero et al., 2007)
Ash	—	
Specific heat [J/kg K]		
Moisture: c_{pm}	4200	(Portiero et al., 2007)
Dry wood: c_{pw}	$103.1 + 3.87\,T_s$	(Hagge and Bryden, 2002)
Char: c_{pc}	$1390 + 0.36\,T_s$	(Hagge and Bryden, 2002)
Ash: c_{pa}	800	(Shin and Choi, 2000)
Pyrolysis reaction rates		
A_{v1} [1/s]	1.30×10^8	(Chan et al., 1985)
E_{v1} [kJ/mol]	140	(Chan et al., 1985)
A_t [1/s]	2.00×10^8	(Chan et al., 1985)
E_t [kJ/mol]	133	(Chan et al., 1985)
A_c+ [1/s]	1.08×10^7	(Chan et al., 1985)
E_c+ [kJ/mol]	121	(Chan et al., 1985)
A_{v2} [1/s]	4.28×10^6	(Liden et al., 1988)
E_{v2} [kJ/mol]	107.5	(Liden et al., 1988)
Char oxidation rate		
A_c [1/(Pa.s)]	8620	(Zhou et al., 2005)
T_{ac} [K]	15900	(Zhou et al., 2005)
Enthalpy of reactions [J/kg]		
Drying	2.25×10^6	(Collazo et al., 2012)
Pyrolysis	418×10^3	(Chan et al., 1985)
	40×10^3	(Liden et al., 1988)
Char oxidation	-250×10^6	(Okuga, 2007)

Table 3 Main properties of the gas, thermal parameters, dynamic viscosity, and diffusion coefficient of O_2 in N_2

Parameter	Value	Reference
Thermal conductivity: $\kappa_g\,[\mathrm{W/mK}]$	$4.8 \times 10^{-4}\, T_g^{0.717}$	(Zhou et al., 2005)
Dynamic viscosity: v_g [Pa s]	$1.98 \times 10^{-5} \left(\frac{T_g}{300}\right)^{2/3}$	(Zhou et al., 2005)
Diffusion coefficient: $D_{O_2-N_2}\,[\mathrm{m^2/s}]$	$2.593 \times 10^{-6}\, T_g^{0.5}$	(Portiero et al., 2007)
Specific heat [J/kg K]:		
Water	$1666 + 0.622\, T_g$	(Shin and Choi, 2000)
Oxygen	$854.7 + 0.2178\, T_g$	(Shin and Choi, 2000)
Nitrogen	$980 + 0.2\, T_g$	(Shin and Choi, 2000)
Carbon dioxide	$708 + 0.4789\, T_g$	(Shin and Choi, 2000)
Carbon monoxide	$977.4 + 0.2\, T_g$	(EngineeringToolbox, 2013)
Volatiles	$0.761 + 7 \times 10^{-4}\, T_g - 2 \times 10^{-7}\, T_g^2$	(Haseli et al., 2011)
Tar	$-0.162 + 4.6 \times 10^{-3}\, T_g - 2 \times 10^{-6}\, T_g^2$	(Haseli et al., 2011)

Heat Transfer

The fuel particles are considered to be thermally thin, i.e., having uniform temperature across their diameter, thus internal thermal gradients are neglected. It is assumed that the particles exchange heat between them by conduction and with their surroundings by convection and radiation mechanisms. The correspondin volumetric heat transfer rates are listed in Table 1, Eqs. (23)–(25).

As can be seen from Table 1, the conductive rate includes an effective thermal conductivity, κ_{eff}. For the solid phase, this parameter is estimated here to be the sum of a conductive and a radiative component:

$$\kappa_{eff} = (1 - \epsilon_b)\,(Y_m \kappa_m + Y_w \kappa_w + Y_c \kappa_c) + \frac{16\sigma\epsilon_b}{3\beta} T_s^3 \tag{13}$$

where $Y_i\,(i = m, w, c)$ denotes the mass fractions of moisture, dry wood, and char; $\beta = A_p/2$ is the absorption coefficient of the particle; and σ is the Stefan–Boltzman constant. For the gas phase it is estimated that $\kappa_{eff} = \epsilon_b \kappa_g$ (Yang et al., 2008).

The convective heat transfer between solid and gas phase is written in terms of the heat transfer coefficient $h_t = \left(\kappa_{eff}/d_p\right)\mathrm{Nu}$ where the experimental correlation of Wakao and Kaguei has been used for the Nusselt number (Peters, 2003):

$$\mathrm{Nu} = [1 + 1.5\,(1 - \epsilon_b)]\left[2 + 1.1\mathrm{Re}^{0.6}\,\mathrm{Pr}^{1/3}\right] \tag{14}$$

It is worth noting the coupling of h_t and the convective heat transfer rate [see Eq. (24)] with the particle diameter d_p. According to such expressions, a significant increase of the convective heat transfer rate is expected when reducing the particle size (i.e., during shrinkage of the particles). The same analysis is valid for the mass transfer coefficient κ_d appearing in Eq. (11).

The radiation from the furnace walls plays an important role in igniting and sustaining combustion in the packed bed. In this work the distribution of energy due to radiation in the solid phase is estimated by Eq. (25), where a solid emissivity of $\xi = 0.85$ is assumed (Collazo et al., 2012). Heat transfer by radiation in the gas phase is neglected. The heat released/consumed during the heterogenous reactions, on the other hand, is assumed to be absorbed in the solid phase and calculated as expressed in Eq. (26), Table 1, where R and ΔH denote the rate and the enthalpy of the reaction, respectively (Shin and Choi, 2000).

Shrinkage of Bed Volume

During the solid conversion process on the grate, the mass loss of the fuel results in a shrinking of the particle volume and thus in a decreased bed height. Shrinkage during biomass combustion affects the heat and mass transport within the bed and thus influences significantly the solid conversion rate and the products yields (Di Blasi, 1996; Thunman, 2001). However, for a thermally thin regime, as assumed here, the impact of the shrinkage on both drying and pyrolysis processes can be neglected (Hagge and Bryden, 2002). Hence, the reduction of particle and bed volume is thus associated with the consumption of char by oxidation only. During drying and pyrolysis it is assumed that the particle volume remains constant provided that the release of solid matter leads to an increase of the internal particle porosity (Ashtana et al., 2010; Collazo et al., 2012; Goh et al., 2001).

It is proposed here to evaluate the shrinkage of the control volume centred at z at the instant t as:

$$\frac{V(z,t)}{V_0} = \left(\epsilon_{cs}(z,t) + \epsilon_a^0\right) \tag{15}$$

where the initial ash fraction, ϵ_a^0, is defined as the ratio of the volume occupied by the ash to the initial volume, $\epsilon_a^0 = V_a / V_0$, and the temporal variation of the combustible solid fraction is evaluated from the char consumption rate:

$$\frac{\partial \epsilon_{cs}(z,t)}{\partial t} = -\epsilon_{cs}(z,t)\frac{R_{c^-}}{\rho_c}, \quad \rho_c > 0 \tag{16}$$

It is worth noting that when $t \to 0$ and $t \to \infty$, the combustible solid fraction takes the following limiting values:

$$\epsilon_{cs}(z,t) \underset{t\to 0}{\longrightarrow} \left(1 - \epsilon_a^0\right)$$

$$\epsilon_{cs}(z,t) \underset{t\to \infty}{\longrightarrow} 0$$

From the above and Eq. (15), it can be easily deduced that $V(z,0) = V_0$ and $V(z,\infty) = V_a, \forall z$, which is an expected result.

Gas Flow Through the Bed

Gases released from the conversion process and air coming from the bottom of the bed move upwards through the pore space of the packed bed. Clearly the bed porosity ϵ_b is an important parameter to be considered in estimating the gas velocity as it determines the

space available for fluid flow. By assuming ϵ_b to be isotropic, the interstitial velocity of the gas perpendicular to the grate is here determined from the air flow as:

$$v_g = \frac{\dot{m}_g}{\epsilon_b A \rho_g} \tag{17}$$

In the above equation A is the cross-sectional area of the bed, ρ_g is the gas density, and the flow rate of the air mass is, in general, evaluated as a discrete function of the coordinate x along the grate:

$$\dot{m}_g(x) = \begin{cases} \dot{m}_g^1; & x \in [0, x_1] \\ \vdots & \\ \dot{m}_g^N; & x \in [x_N, L] \end{cases} \tag{18}$$

allowing to model different air flow rates $\dot{m}_g^i$ at different bed bottom sections, $[x_i, x_j]$. Values of $\dot{m}_g^i$ are estimated as a function of design and operational parameters, such as the excess air ratio λ, the boiler efficiency η, and the boiler capacity $\dot{Q}$, according to:

$$\dot{m}_g^i = \left(\frac{32 + 8m - 16n}{12 + m + 16n}\right)\left(\frac{\lambda_i \dot{Q}}{Y_{O_2}^0 \eta}\right)\left(\frac{\left(1 - Y_m^0\right)}{\left(1 - Y_m^0\right) H_{u,dry} - Y_m^0 \Delta h_m}\right) \tag{19}$$

for a fuel assumed to be composed of CH_mO_n. The quantities Y_m^0, Y_w^0, and $Y_{O_2}^0$ denote the initial mass fractions of moisture, dry wood, and oxygen, respectively, whereas Δh_m is the evaporation enthalpy of water and $H_{u,dry}$ is the lower heating value of absolutely dry wood, i.e., at moisture content $Y_m = 0$.

A mapping between the horizontal coordinate x appearing in Eq. (18) and the residence time t of the fuel on the grate is performed provided that the bed moves at a constant velocity (here called moving bed velocity) $u_b : x = u_b t$. The value of u_b is adjusted to experimental results as described in the section, Definition of the Reference Case.

Numerical Solution

The partial differential equations (PDEs) system is solved by using the method of lines (Schiesser, 1991), which decouples the time integration from the spatial discretization by converting the original PDEs into an equivalent system of ordinary differential equations (ODEs) in the variable t. The spatial discretization is performed by using the finite volume method (Pantakar, 1980) with a uniform mesh step size δ_z. The obtained ODEs are advanced in time by using the solver LSODA (Petzold, 1983), which automatically switches between the multi-step Adams method (non-stiff solver) and the implicit backward differentiation (BDF) method (stiff solver) depending on how stiff the system is. In general, when the solution appears to vary rapidly in a particular region, the solver by means of an adaptive procedure reduces the local time step, δ_t, or changes the method to be able to better track the solution.

The values of both spatial and time steps were chosen carefully to meet an accuracy of 10^{-4} for the solutions. The optimum value for the spatial resolution was selected as $\delta z_c = 0.84\, d_p$, with d_p being the particle diameter (i.e., the characteristic length scale), whereas

the time step was allowed to vary locally with magnitudes, $\delta t_c \leq 0.1\,s$. In this way a mesh-independent solution could be obtained and a broad set of input parameters was explored by setting appropriate initial and boundary conditions. Initial conditions were defined by the initial fuel and air properties, while boundary conditions at the bottom and the top of the bed were given by operating conditions (i.e., air velocity, wall temperature, etc.).

RESULTS AND DISCUSSION

Definition of the Reference Case

In order to illustrate the applicability of the proposed model, it is shown how the model allows predicting fuel and operational parameter values at which optimum conditions for the solid fuel conversion on the grate can be achieved. Optimum conditions are assumed if, on the one hand, unburned carbon in the grate ash is avoided. For this, the solid fuel conversion needs to be safely completed on the grate. On the other hand, the uncovered grate area should be as small as possible to avoid undesired primary air intake through these grate zones.

Experiments on a 1.2-MW boiler revealed that optimum conditions for both gas phase oxidation and char burnout can be achieved if the conversion of the solid carbon in the fuel is completed at a grate length of $x = 0.8L$ (Kiener and Nussbaumer, 2012), which for the present work is further defined as optimum fuel conversion condition. Both fuel properties and operational conditions used in Kiener and Nussbaumer (2012) to achieve the target value of 80% grate coverage are taken as a guide to choose a set of input parameters for the calculations (see Table 4) defined as the reference case in the present study. In the calculation, the bed velocity u_b is adjusted to a fixed value in order to achieve 80% grate coverage. For the calculated cases presented here, the grate velocity is kept constant at $u_b = 0.0009$ m/s, which corresponds to a residence time of non-combustible material, such as ash, on the grate of 37 min.

Figure 2 illustrates the distribution of the mass fraction of char on a grate of length $L = 2$ m. The reference case, i.e., case (a) in Figure 2, shows the result obtained for the parameters listed in Table 4 with the combustible zone ending at a normalized grate length $\hat{x} = 0.8$, thus fulfilling the desired condition and leading to a remaining layer of nearly pure ash on the last section of the grate.

Table 4 Main input parameters used for generating the reference case displayed in Figure 2a

Parameter	Symbol	Value
Boiler efficiency	η	0.85
Boiler capacity	$\dot{Q}$	1.2 MW
Excess air ratio[a]	λ	0.7
Wall temperature	T_{wall}	1290 K
Primary air temperature	T_{PA}	320 K
Bed porosity	ϵ_b	0.55
Particle diameter	d_p	12 mm
Initial moisture mass fraction	Y_m^0	0.3
Initial ash mass fraction	Y_a	0.02
Initial dry wood density	ρ_w^0	558 kg/m^3
Moving bed velocity	u_b	0.0009 m/s

[a]Here, the excess air ratio on the grate, i.e., the primary excess air ratio, is regarded.

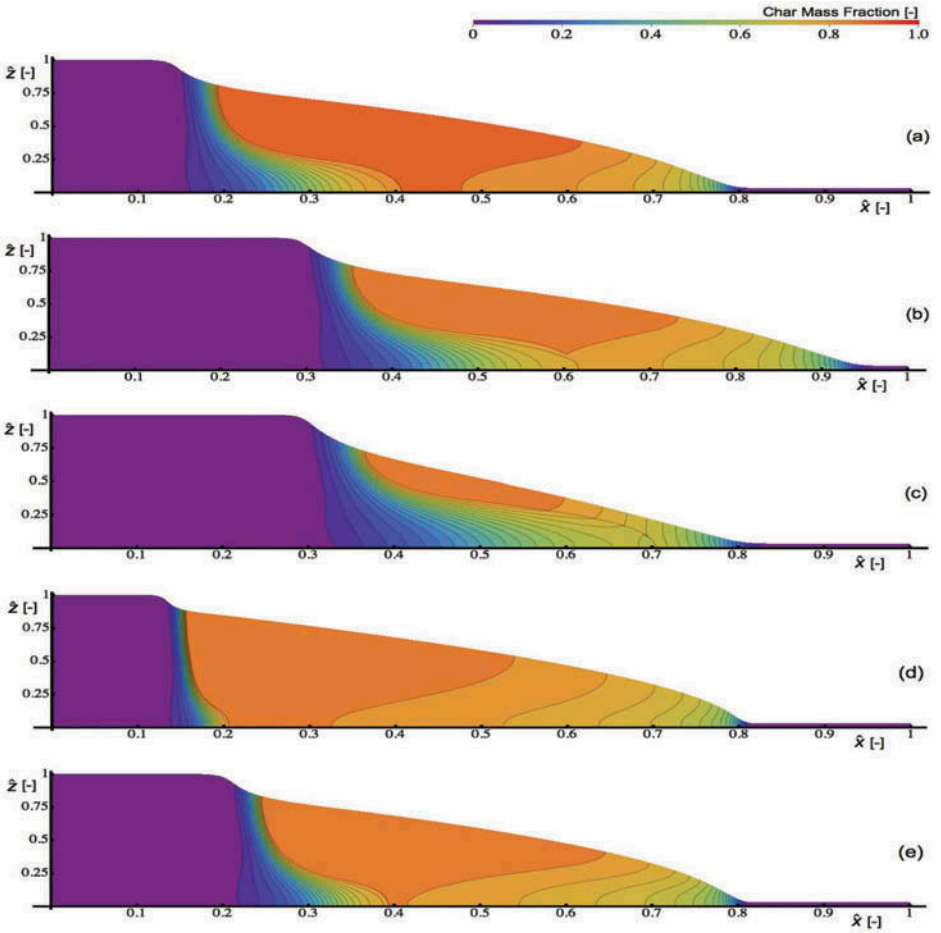

Figure 2 Solid fuel conversion on the grate shown by char mass fraction. $\hat{x} = x/L$ and $\hat{z} = z/H_0$, with L and H_0 being the grate length and the initial bed height, respectively: $(H_0/L) = 0.2$. (a) Reference case calculated with input parameters listed in Table 4. (b) Same as (a) but with 50% moisture instead of 30%. (c) Same as (b) but with $\lambda = 1$ instead of $\lambda = 0.7$. (d) Same as (b) but with 45% load instead of 100% (boiler capacity 0.54 MW instead of 1.2 MW). (e) Same as (b) but with pre-heated primary air with $T_{PA} = 390$ K instead of 320 K.

Influence of Moisture Increase on Solid Fuel Conversion at Constant Operation Parameters

To investigate the influence of the moisture content on the combustion, the moisture content is varied while keeping all other parameters constant. Figure 2b shows the effect of a moisture increase from 30% to 50% on the char distribution on the grate. The moisture increase initially leads to a reduction of the adiabatic flame temperature in the gas phase above the grate and consequently to a reduced temperature of the ceiling of the combustion chamber (T_{wall}). Due to the increased time and space needed for fuel drying and water evaporation and due to the reduced ceiling temperature, the conversion of the solid fuel to gases is decelerated and the fuel bed volume increases compared to the reference case. Consequently, combustible matter is transported almost to the end of the grate, which can

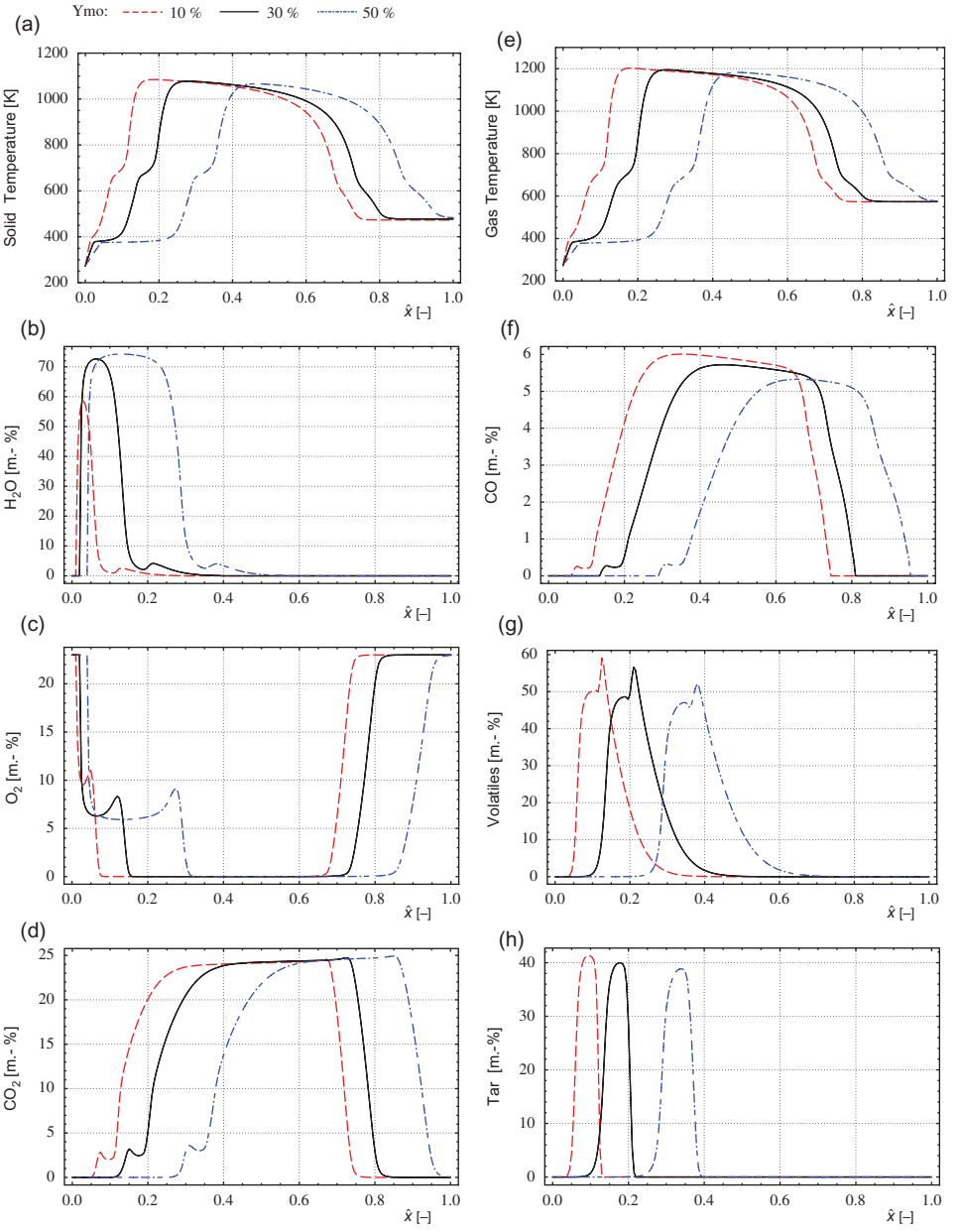

Figure 3 Influence of fuel moisture content: Solid temperature, gas temperature, and gas species at the bed surface as function of the grate length for the reference case (moisture content 30%) and for a moisture content of 10% and 50% with other parameters as listed in Table 4. $\hat{x} = x/L$.

result in unburned carbon in the grate ash and is hence an undesired operation mode. This deceleration effect is also clearly manifested in the gas distribution resulting from the solid conversion process, as shown in Figure 3, displaying the calculated gas profiles for H_2O, O_2, CO_2, CO, volatiles and tar species released at the top of the bed. As can be seen from

the gas profiles, an increased moisture content leads to a shift of the gas release towards the end of the grate. Gas profiles obtained at 30% (thick black line in Figure 3) and 50% (dot-dashed blue line in Figure 3) moisture content correspond to the char distributions displayed in Figures 2a and 2b, respectively. Furthermore, Figure 3 shows the effect of a reduced moisture content with a shift of the gas release towards the first section of the grate. Simultaneously, this results in a reduced fuel bed length on the grate with a significantly increased uncovered grate as further discussed in the last sub-section of the Results and Discussion section.

As a consequence of the isothermal approximation of the particles, the calculation can lead to an underestimation of the width of the reaction front as described in the Modeling Approach section. Therefore, the profiles for solid and gas temperatures as predicted in Figures 3a and 3e can potentially appear steeper than expected in reality and also the steep gradient with a narrow peak as predicted for tar in Figure 3h is presumably overestimated.

Variation of Operation Parameters to Recover Optimum Conditions at Increased Fuel Humidity

The phenomenon of the influence of fuel moisture on the grate coverage described above is known from practical experience and leads to an undesired operation unless the boiler parameters are adapted to the varying moisture content (Kiener and Nussbaumer, 2012). Hence, it is of interest to predict the effect of operation parameters on the solid fuel conversion. Since the present model allows to predict the fuel conversion for a given set of operation parameters, it enables to find further sets of parameters achieving optimum conditions by iteration, i.e., by varying one single parameter, which enables to recover the desired conditions. To illustrate the capability of the model, the following operation parameters are varied to find new boiler settings enabling to recover optimum conditions at elevated moisture content:

- Figure 2c: Excess air ratio.
- Figure 2d: Boiler capacity.
- Figure 2e: Primary air temperature (e.g., by pre-heating).

As shown in Figure 2, ideal combustion conditions can be recovered at increased moisture if one of the three investigated parameters is changed as follows:

- Increasing the primary excess air ratio from 0.7 to 1.0 (Figure 2c).
- Reducing the boiler capacity from 1.2 MW to 0.54 MW corresponding to a reduction from 100% to 45% (Figure 2d).
- Preheating the primary air from 320 K to 390 K (Figure 2e).

While all three operation modes enable to recover the optimum fuel bed length, they also affect the temperature profiles and the gas release from the solid fuel. However, each measure affects the combustion situation differently, with the following effects as illustrated in Figure 4.

Effect of primary air temperature. While all investigated cases show a clear drying section at the beginning of the grate (identified by the release of water vapor in graph (b)), the length of the drying zone and the vapor content in the gas vary. In comparison to the reference case, the air preheating (at increased moisture) results in an enhanced drying on

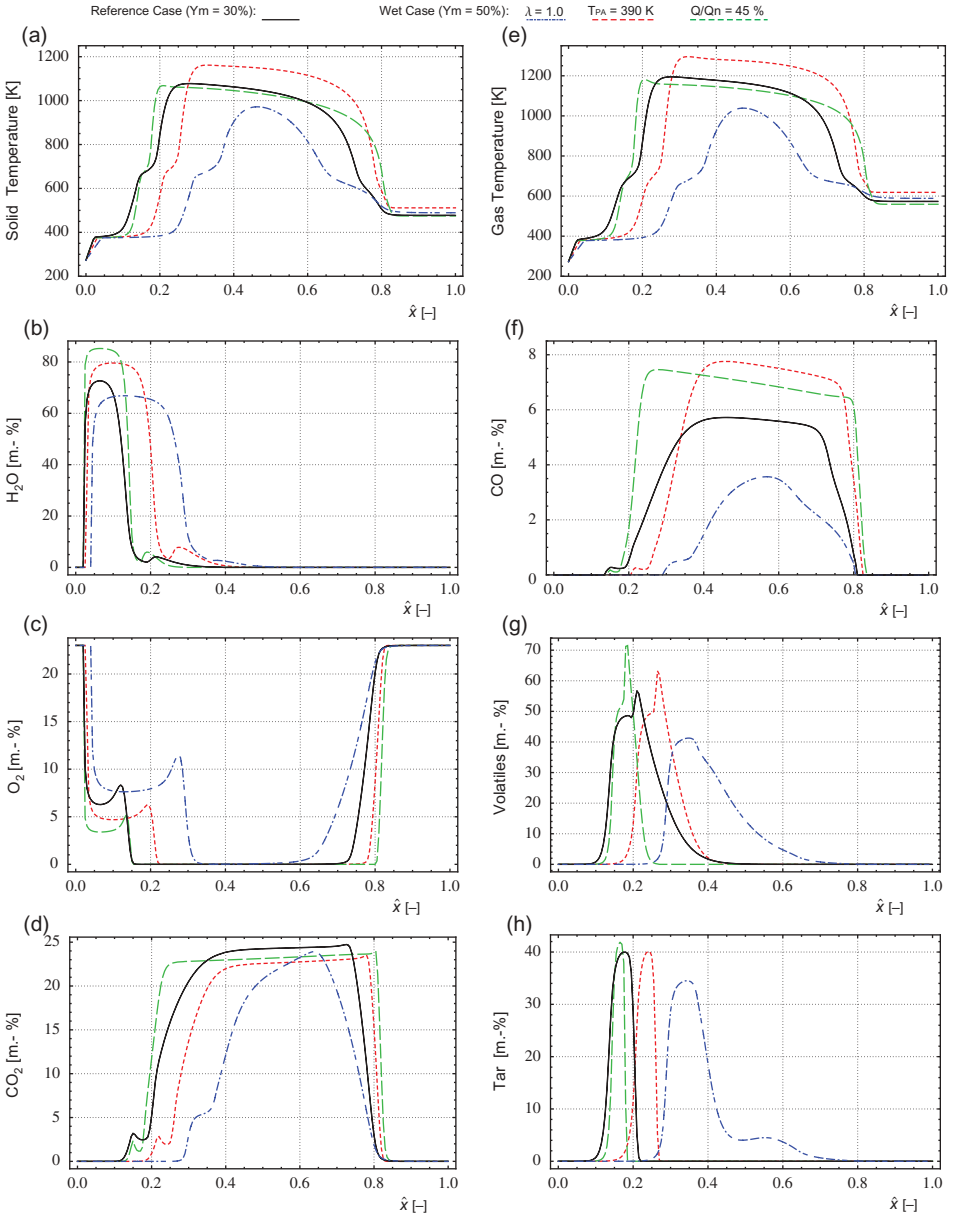

Figure 4 Influence of operation parameters on solid temperature, gas temperature, and released gas species as function of the grate length. The graphs show the following four cases: The reference case (black line) and the three cases with increased fuel moisture and change of one single operation parameter enabling to recover optimum solid fuel conversion conditions on the grate, i.e., $\lambda = 1.0$ (dot dashed blue line), primary air temperature $T_{PA} = 390\,\mathrm{K}$ (dashed red line), and 50% boiler load (dashed green line). $\hat{x} = x/L$.

the first grate section with slightly increased vapor content. However, due to the increased fuel humidity, the total water release takes more time and space as can be seen by the total water released from the fuel and indicated by the area below the concentration of water vapor (graph (b)). Consequently, the end of the drying is shifted forward in the direction of

the grate. However, after completion of the drying, significantly higher temperatures of both solid and gas phases are achieved due to the increased air temperature as shown in graph (e). Thanks to an increased temperature, the solid fuel conversion to CO_2, CO, volatiles, and tar is accelerated as can be seen, e.g., by the shorter but higher peak of volatile release. This accelerated solid fuel conversion finally enables the completion of the char conversion at the same grate length as in the reference case despite the prolonged initial drying section.

Effect of load. Reduced load at increased fuel humidity results in fairly similar profiles as the reference case for both gas temperatures and gas species. This is due to the fact that the total amount of water vapor is slightly reduced compared to the reference case (due to the reduced fuel rate) and, hence, does not take significantly more space on the grate since drying is supported by the nearly constant heat transfer from the ceiling (being proportional to the heat transfer area). Given that, after drying the conversion of dry wood occurs, the resulting gas temperature above the fuel bed is only slightly lower than the temperature achieved in the reference case. It should be noted that due to the energy conservation, the adiabatic temperature in the post combustion chamber is reduced significantly, which, however, does not affect the solid fuel conversion.

Effect of primary excess air ratio. At increased fuel moisture and increased excess air, the vapor content in the gas is reduced due to the increased dilution with air, which also results in an increased oxygen concentration in the gas mixture released from the drying zone (graphs (b) and (c)). Due to the increased amount of released water, the drying zone is significantly prolonged, and the start of the fuel conversion is consequently shifted towards the middle of the grate. Due to the increased amount of air available in the main gasification zone, a higher proportion of the heating value of the fuel is released on the grate. This results in an accelerated fuel conversion, which consequently again enables a complete char conversion at the same grate length as in the reference case. However, due to the dilution of the released gases with additional nitrogen from the combustion air, the temperature of solids and gases are lower than in the reference case (graphs (a) and (e)). This effect also needs to be considered when comparing the combustion progress and the resulting gas concentrations, which are significantly lower than in the reference case due to the dilution (graphs (d), (f), and (g)). On the other hand, the reduced temperature during the solid fuel conversion results in an increased tar release from the fuel bed as shown in graph (h).

Influence of Operation Parameters on Fuel Bed Length

Instead of using the model to identify optimum conditions by iteration as described in the previous section, it can also be applied to predict the expected fuel bed length as function of different sets of both fuel and operation parameters. For this, Figure 5 shows the normalized bed length as function of the moisture content for different primary excess air ratios and different boiler loads. A horizontal line at $\left(\hat{x} = 0.8\right)$ indicates the target value of the fuel bed length. At nominal load and a moisture content of 30%, this condition is met by the reference case (a) indicated in the graph at the top in Figure 5.

In this graph, case (b) described in the previous section corresponds to an increase of the fuel humidity to 50% at identical operation parameters. For this situation, the model predicts a fuel bed length of approximately 95% as described above and, hence, indicates an undesired operation mode. As shown by data point (c) in the graph, recovering optimum conditions is predicted by an increase of the primary excess air ratio from 0.7 to 1.0 corresponding to the situation described in the previous section.

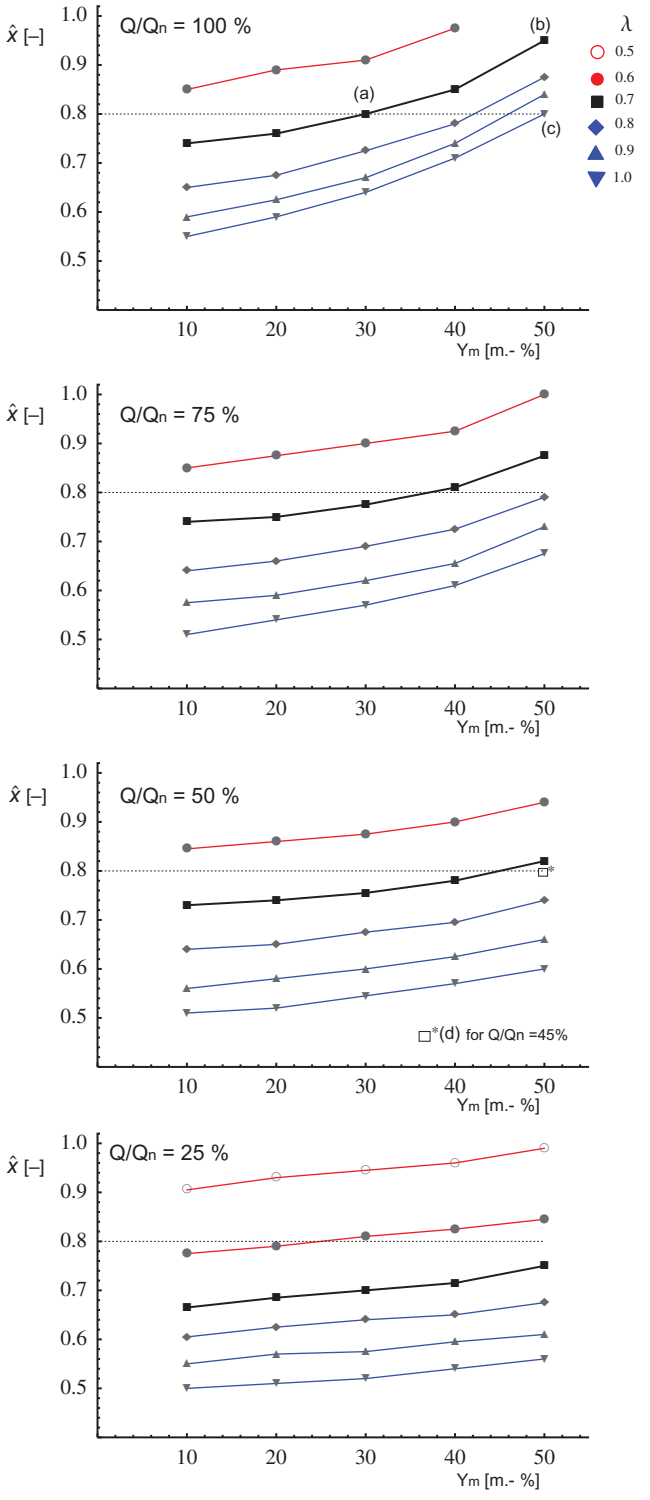

Figure 5 Calculated dimensionless bed length $(\hat{x} = x/L)$ as a function of the fuel moisture content Y_m for different excess air ratios λ and boiler loads. Points labeled (a), (b), (c), and (d) represent the cases illustrated in Figures 2a, 2b, 2c, and 2d, respectively.

Since the boiler capacity is usually not applicable as a control variable, the figures showing the fuel bed geometry for reduced load can be used to predict the optimum set point for the combustion control system, here shown by the example of the primary excess air as potential control variable. Consequently, the results predict the following conditions to achieve optimum conditions for some examples:

- At 25% load and constant moisture content of 30%, a reduction of the primary excess air from 0.7 to 0.6 is proposed (see graph at 25% load, i.e., bottom).
- At 75% load and 40% moisture content, a primary excess air of 0.7 (hence, being identical as for the reference operation) is proposed.
- With increased moisture content, the optimum conditions can be recovered by increasing the primary excess air. As shown in the graph for 50% load, optimum conditions at 50% load are predicted for a moisture content of approximately 44%. From the graph it can be estimated that, for 50% moisture content, optimum conditions are achieved at approximately 45% load as indicated by the data point (d). This operation mode corresponds to case (d) described in the preceding section.

CONCLUSIONS

A comprehensive model for the solid fuel conversion on a grate is developed, which describes most of the physical-chemical and thermal phenomena involved during fuel combustion: mass and heat transfer between the solid and gas phases, gas flow, drying, pyrolysis, char oxidation, and reduction of the bed volume. All this phenomena were described on the basis of models and kinetic data reported and validated in the literature.

The model enables the calculation of the conversion of a moisture and ash containing solid fuel with a specific particle size on a grate to water vapor, tar, and volatiles released from the fuel bed, and remaining char and ash on the grate, and to predict the temperatures of gases and solids. By doing so, the model can be applied to predict the influences of varying fuel properties, such as moisture content, particle size, and ash content, as well as influences of operating conditions, such as local excess air and primary air temperature on the solid fuel conversion.

The simulation of a reference case achieving optimized conditions on the grate for both burnout quality of the grate ash and avoiding undesired air leakage through uncovered grate sections is defined based on experiences from real-life operation of grate boilers. Therefrom, optimum conditions are assumed if the solid fuel conversion to nearly pure ash ends at a dimensionless grate length of 0.8. Based on this, the model allows to predict the influence of a variation of one or more parameters and to identify boiler settings for specifically defined ideal grate operation conditions (here presented for the example of a finalized conversion at 80% grate length). This is of specific interest to predict the influence of varying fuel properties, such as the moisture content and/or load conditions.

Example calculations show that an increasing fuel moisture leads to unburned carbon in the grate ash in case of constant boiler settings and if starting from an optimized combustion situation at nominal boiler capacity. However, ideal combustion conditions can be recovered, e.g., by one of the following measures:

1. Increase of the excess air ratio, or
2. reduction of the boiler capacity, or
3. preheating of the primary air.

For practical purposes, all investigated operation parameters also influence other parameters than the solid fuel conversion and cannot always be independently applied or controlled. For practical applications, the following effects need to be considered:

1. An increase of the primary excess air is theoretically applicable and most often available as a potential measure in practical applications. However, the boiler design needs to be capable to fulfill certain requirements, such as an increase of the primary air flow. In addition, the secondary air needs to be reduced, thus potentially affecting the flow situation in the post combustion chamber. In addition, the implementation of a precise control system requires measurement, e.g., of the boiler capacity and the primary air flow.
2. A reduction of the boiler capacity does not need additional technical measures with respect to the boiler and the control system; however, it is usually not applicable as an independent control variable and, hence, is only used as a measure in case of lack of other measures to avoid unburned carbon in the residues.
3. Preheating of the primary air can be implemented as a technical measure and is applicable if considered in the design and planning phase. For such applications, the results from the model can be used to optimize the process control by predicting ideal set points. However, since the applicable range of air-preheating is usually limited, flue gas recirculation is often applied as an additional measure enabling an expansion of the control regime.

Besides the independent application of one of the three investigated measures, two or more measures can be combined and further measures, such as flue gas recirculation, can be evaluated with the present model.

Based on these findings, the model is proposed as a useful tool to investigate the influence of operation and design parameters on the solid fuel conversion on a grate and to derive information on concepts and ideal set-points for combustion control concepts. In addition, the model can be coupled to the consecutive gasphase reactions in the combustion chamber enabling modeling by computational fluid dynamics (CFD) as applied, e.g., in Nussbaumer and Kiener (2013). Furthermore, model runs will be expanded for additional operation parameters, such as bulk density and particle size, of the investigated fuels. Moreover, the empiric data from the literature used as basis for the presented simulations will be validated by measurements of gas species and temperature profiles above the fuel bed in a moving grate boiler.

REFERENCES

Ashtana, A., Yannick, M., Sessiecq, P., and Patisson, F. 2010. Modeling on-grate MSW incineration with experimental validation in a batch incinerator. *Ind. Eng. Chem. Res.*, **49**, 7597–7604.

Bruch, C., Peters, B., and Nussbaumer, T. 2002. Modelling wood combustion under fixed bed conditions. *Fuel*, **82**, 729–738.

Chan, W.C., Kelbon, M., and Krieger, B.B. 1985. Modelling and experimental verification of physical and chemical processes during pyrolysis of large biomass particles. *Fuel*, **64**, 1505–1513.

Collazo, J., Portiero, J., Patiño, D., and Granada, E. 2012. Numerical modeling of the combustion of densified wood under fixed–bed conditions. *Fuel*, **93**, 149–159.

Di Blasi, C. 1993. Modeling and simulation of combustion processes of charring and non-charring solid fuels. *Prog. Energy Combust. Sci.*, **19**, 71–104.

Di Blasi, C. 1996. Heat, momentum and mass transport through a shrinking biomass particle exposed to thermal radiation. *Chem. Eng. Sci.*, **51**, 1121–1132.

Di Blasi, C. 2004. Modeling wood gasification in a countercurrent fixed-bed reactor. *AIChE J.*, **50**, 2306–2319.

EngineeringToolbox. 2013. Specific heat of carbon monoxide gas -CO- at temperatures ranging 175–6000 K. The Engineering ToolBox. Available at: http://www.engineeringtoolbox.com/carbon-monoxided_975.html.

Essenhigh, R.H., and Kuo, T.J. 1970. Combustion and emission phenomena in incinerators: Development of physical and mathematical models of incinerators, Part I: Statement of the problem. In *Proceedings of the National Incinerator Conference*, ASME, New York, pp. 261–271.

Goh, Y.R., Siddall, R.G., Nasserzadeh, V., Zakaria, R., Swithenbank, J., Lawrence, D., Garrod, N., and Jones, B. 1998. Mathematical modelling of the waste incinerator burning bed. *J. Inst. Energy*, **71**, 110–118.

Goh, Y.R., Yang, Y.B., Zakaria, R., Siddall, R.G., Nasserzadeh, V., and Swithenbank, J. 2001. Develpment of an incinerator bed model for municipal solid waste incineration. *Combust. Sci. Technol.*, **162**, 37–58.

Hagge, M.J., and Bryden, K.M. 2002. Modeling the impact of shrinkage on the pyrolysis of dry biomass. *Chem. Eng. Sci.*, **57**, 2811–2823.

Haseli, Y., van Oijen, J.A., and de Goey, L.P.H. 2011. Modeling biomass particle pyrolysis with temperature-dependent heat of reactions. *J. Anal. Appl. Pyrolysis*, **90**, 140–154.

Johansson, R., Thunman, H., and Leckner, B. 2007. Influence of intraparticle gradients in modeling of fixed bed combustion. *Combust. Flame*, **149**, 49–62.

Kær, S.K. 2004a. Numerical modelling of a straw-fired grate boiler. *Fuel*, **83**, 1183–1190.

Kær, S.K. 2004b. Straw combustion on slow-moving grates—A comparison of model predictions with experimental data. *Biomass Bioenergy*, **28**, 307–320.

Kiener, M., and Nussbaumer, T. 2012. Influence of uneven fuel distribution on a grate on gas flow conditions and combustion quality. Presented at the 20th European Biomass Conference and Exhibition, Milan, Italy, June 18–22, pp. 1112–1117.

Liden, A.G., Berruti, F., and Scott, D.S. 1988. A kinetic model for the production of liquids from the flash pyrolysis of biomass. *Chem. Eng. Commun.*, **65**, 207–221.

Lu, H., Robert, W., Peirce, G., Ripa, B., and Baxter, L.L. 2008. Comprehensive study of biomass particle combustion. *Energy Fuels*, **22**, 2826–2839.

Nussbaumer, T., and Kiener, M. 2013. Moving grate combustion optimisation with CFD and PIV. Presented at the 21st European Biomass Conference and Exhibition, Cophenhagen, Denmark, June 3–7, pp. 1112–1117.

Okuga, A. 2007. Analysis and operability optimization of an updraft gasifier unit. Master thesis. Department of Mechanical Engineering, Eindhoven University of Technology, Eindhoven, Netherlands.

Pantakar, S. 1980. *Numerical Heat Transfer and Fluid Flow*, Hemisphere, New York.

Peters, B. 2002. Measurements and application of a discrete particle model (DPM) to simulate combustion of a packed bed of individual fuel particles. *Combust. Flame*, **131**, 132–146.

Peters, B. 2003. *Thermal Conversion of Solid Fuels*, WIT Press, Southampton, UK.

Peters, B., and Bruch, C. 2003. Drying and pyrolysis of wood particles: Experiments and simulation. *J. Anal. Appl. Pyrolysis*, **70**, 233–250.

Petzold, L.R. 1983. Automatic selection of methods for solving stiff and nonstiff systems of ordinary differential equations. *J. Sci. Stat. Comput.*, **4**, 136–148.

Portiero, J., Granada, E., Patiño, D., and Morán, J.C. 2007. A model for the combustion of large particles of densified wood. *Energy Fuels*, **21**, 3151—3159.

Schiesser, W.E. 1991. *The Numerical Method of Lines*, Academic Press, San Diego, CA.

Schlünder, E.U., and Tsotsas, E. 1988. *Wärmeübertragung in Festbetten, Durchmischten Schüttungen und Wirbelschichten*, Thieme Verlag, Stuttgart.

Schroer, K., Guillmann, P., and Görner, K. 2008. *Probleme beim Einsatz von Ersatzbrennstoffen in Kleinen Dezentralen Anlagen*, Deutscher Flammentag, Berlin.

Shin, D., and Choi, S. 2000. The combustion of simulated waste particles in a fixed bed. *Combust. Flame*, **121**, 167–180.

Thunman, H. 2001. Principles and models of solid fuel combustion. PhD thesis. Department of Energy Conversion, Chalmers University of Technology, Göteborg, Sweden.

Troccia, N., Palmeri, F., and Gallucci, F. 2012. Combustion modeling of a biomass packed bed in moving grate furnaces. Presented at the 20th European Biomass Conference and Exhibition, Milan, Italy, June 18–22, pp. 1276–1285.

Van der Lans, R.P., Pedersen, L.T., Jensen, A., Glarbog, P., and Dam-Johansen, K. 2000. Modelling and experiments of straw combustion in a grate furnace. *Biomass Bioenergy*, **19**, 199–208.

Wakao, N., and Funazkri, T. 1978. Effect of fluid dispersion coefficients on particle-to-fluid mass transfer coefficients in packed beds: Correlation of sherwood numbers. *Chem. Eng. Sci.*, **33**, 1375–1384.

Yang, Y.B., Goh, Y.R., Zakaria, R., Nasserzadeh, V., and Swithenbank, J. 2002. Mathematical modelling of MSW incineration on a travelling bed. *Waste Manage.*, **22**, 369–380.

Yang, Y.B., Ryu, C., Goodfellow, J., Shafiri, V.N., and Swithenbank, J. 2004. Modelling waste combustion in grate furnaces. *Trans. IchemE, Part B*, **82**(B3), 208–222.

Yang, Y.B., Ryu, C., Khor, A., Yates, N.E., Sharifi, V.N., and Swithenbank, J. 2005a. Effect of fuel properties on biomass combustion. Part II. Modelling approach-identification of the controlling factors. *Fuel*, **84**, 2116–2130.

Yang, Y.B., Sharifi, V.N., and Swithenbank, J. 2005b. Numerical simulation of the burning characteristics of thermally-thick biomass fuels in packed-beds. *Trans. IchemE, Part B*, **83**(B6), 549–558.

Yang, Y.B., Sharifi, V.N., Swithenbank, J., Ma, L., Darvell, L.I., Jones, J.M., Pourkashanian, M., and Williams, A. 2008. Combustion of a single particle of biomass. *Energy Fuels*, **22**, 306–316.

Zhou, H., Jensen, A.D., Glarborg, P., Jensen, P.A., and Kavaliauskas, A. 2005. Numerical modeling of straw combustion in a fixed bed. *Fuel*, **84**, 389–403.